Plectranthus amboinicus Attenuates Inflammatory Bone Erosion in Mice with Collagen-induced Arthritis by Downregulation of RANKL-induced NFATc1 Expression

YU-CHIEH HSU, CHIA-PI CHENG, and DEH-MING CHANG

ABSTRACT. ***Objective.*** *Plectranthus amboinicus* has been known to treat inflammatory diseases or swelling symptoms. We investigated whether *P. amboinicus* exhibited an inhibitory effect on osteoclastogenesis *in vitro* and inflammatory bone erosion in collagen-induced arthritis (CIA) mice, an animal model of rheumatoid arthritis. We attempted to identify the active component of *P. amboinicus* involved in regulation of osteoclastogenesis.

Methods. We treated M-CSF- and RANKL-stimulated murine bone marrow-derived macrophages (BMM) and RANKL-induced RAW264.7 cells with different concentrations of *P. amboinicus* or rosmarinic acid, a phytopolyphenol purified from *P. amboinicus*, to monitor osteoclast formation by TRAP staining. The mechanism of the inhibition was studied by biochemical analysis such as RT-PCR and immunoblotting. CIA mice were administered gavages of *P. amboinicus* (375 mg/kg) or placebo. Then clinical, histological, and biochemical measures were assessed to determine the effects of *P. amboinicus* on synovial inflammation and bone erosion by H&E staining of the inflamed joints and ELISA.

Results. Rosmarinic acid strongly inhibited RANKL-induced NF-κB activation and nuclear factor of activated T cells c1 (NFATc1) nuclear translocation in BMM, and also inhibited RANKL-induced formation of TRAP-positive multinucleated cells. A pit formation assay and the CIA animal model showed that *P. amboinicus* significantly inhibited the bone-resorbing activity of mature osteoclasts.

Conclusion. We postulated that rosmarinic acid conferred the inhibitory activity on *P. amboinicus* for inhibition of osteoclastogenesis via downregulation of RANKL-induced NFATc1 expression. Our results indicated the possibility of *P. amboinicus* as a new remedy against inflammatory bone destruction. (First Release July 1 2011; J Rheumatol 2011;38:1844–57; doi:10.3899/jrheum.101223)

Key Indexing Terms:
COLLAGEN-INDUCED ARTHRITIS
OSTEOCLAST
PLECTRANTHUS AMBOINICUS
NUCLEAR FACTOR OF ACTIVATED T CELLS c1

From the Departments of Rheumatology/Immunology/Allergy, National Defense Medical Center, Taipei; Graduate Institute of Medical Sciences, National Defense Medical Center, Taipei; and Departments of Rheumatology/Immunology/Allergy, Tri-Service General Hospital, National Defense Medical Center, Taipei, Taiwan, Republic of China.

Supported by the National Science Council, Taiwan (NSC-97-2628-B-016-001-MY3 and NSC-99-2628-B-016-001-MY3 to Dr. Chang) and by Tri-Service General Hospital, National Defense Medical Center, Taipei, Taiwan, Republic of China (TSGH-C99-007-S01 and TSGH-C100-005-007-8-S01).

Y-C. Hsu, MS, Departments of Rheumatology/Immunology/Allergy, National Defense Medical Center; C-P. Cheng, PhD, Graduate Institute of Medical Sciences, National Defense Medical Center; D-M. Chang, MD, PhD, Departments of Rheumatology/Immunology/Allergy, Tri-Service General Hospital, National Defense Medical Center.

Address correspondence to Dr. D-M. Chang, Rheumatology/Immunology/Allergy, Tri-Service General Hospital, National Defense Medical Center, 161 MinChuan E. Road, Sec. 6, Neihu 114, Taipei, Taiwan, Republic of China. E-mail: ming0503@ms3.hinet.net

Accepted for publication June 1, 2011.

Rheumatoid arthritis (RA) is a chronic inflammatory autoimmune disease characterized by the presence of synovitis, bone erosion concomitant with pannus formation, and the destruction of joint cartilage[1,2,3,4]. An increasing body of evidence has demonstrated that osteoclasts play a pivotal role in the bone resorption in inflammatory joint diseases. Multinucleated giant cells with the phenotypic features of osteoclasts predominate at erosion sites in RA and animal models of collagen-induced arthritis. Further, it has been reported that mice lacking osteoclasts were resistant to arthritis-induced bone erosion[5]. These findings indicate the application of herbal compounds that inhibit osteoclastogenesis at inflammatory sites might be promising in treatment of RA. However, no study has to date reported the regulatory effects of *Plectranthus amboinicus* on osteoclastogenic differentiation.

Bone mass in adults is intricately regulated by a balance between osteoclast-mediated bone resorption and osteoblast-induced bone formation[6,7]. Perturbations in this balance lead to diseases such as osteoporosis caused by an abnormally high bone metastasis with enhanced bone-resorbing activity of osteoclasts. Therefore, upregulated activation of osteoclasts is the target for therapeutic intervention in pathological bone loss. The differentiation into multinucleated osteoclasts from hematopoietic monocyte/macrophage precursor cells requires 2 cytokines, macrophage colony-stimulating factor (M-CSF) and receptor activator of nuclear factor-κB (NF-κB) ligand (RANKL)[8]. Osteoblasts produce these 2 cytokines in membrane-bound or secreted form when activated by interleukin 1 (IL-1), prostaglandin E_2, and vitamin D3[9,10,11]. RANKL expressed in osteoblasts is the key cytokine involved in the differentiation from precursor cells into osteoclasts, whereas M-CSF secreted by osteoblasts provides a survival signal for osteoclasts. Binding of RANKL to its receptor RANK activates tumor necrosis factor (TNF) receptor-associated factor 6 (TRAF6)[12,13], which is critical for the RANK-induced activation of the NF-κB and mitogen-activated protein kinases (MAPK). Active extracellular signal-regulated kinase (ERK) can directly phosphorylate c-Fos and active c-Jun-N-terminal kinase (JNK) phosphorylates c-Jun[14,15,16]. Thus AP-1 transcription factor, a heterodimer composed of a Fos family (c-Fos, FosB, Fra-1, Fra-2) and a Jun family (c-Jun, JunB, JunD) protein, can be a target of ERK and JNK in response to RANKL in osteoclast precursor cells. In addition, nuclear factor of activated T cells c1 (NFATc1), the key transcription factor for osteoclastogenesis, is strongly induced by RANKL. Accumulating evidence suggests that NFATc1 directly regulates some osteoclast-specific genes such as *TRAP*, *calcitonin receptor*, *cathepsin K*, *β3 integrin*, and *OSCAR*[17].

P. amboinicus is known as a medicinal plant that has been used for abrasions and lacerations, for burns, coughs and colds, and also for conjunctivitis. The major components of *P. amboinicus* as an aqueous extract are Δ-3-carene, γ-terpinene, camphor, and carvacrol[18]. In Taiwan, *P. amboinicus* is a folk herb used to treat inflammatory diseases or swelling symptoms[19]. A recent study revealed that treatment with *P. amboinicus* mitigated the arthritic severity in collagen-induced arthritis (CIA) rats[20]. However, how *P. amboinicus* is involved in the regulation of inflammatory bone erosion in CIA remains elusive.

We assessed the effects of *P. amboinicus* and rosmarinic acid (RosA), a phytopolyphenol, on RANKL-induced osteoclastogenesis in RAW 264.7 cells and bone marrow-derived macrophages (BMM). Moreover, we evaluated the *in vivo* efficacy of *P. amboinicus* in CIA mice to make a direct comparison with *in vitro* data obtained in the analog preparation from BMM.

MATERIALS AND METHODS

Mice and reagents. DBA/1J mice were purchased from the Jackson Laboratory and bred under conventional conditions at the Animal Center of the National Defense Medical Center, Taiwan. All experimental procedures were approved by the Institute Animal Care and Use Committee in Taiwan. The murine monocyte/macrophage RAW 264.7 cell line was obtained from the Food Industry Research and Development Institute, Taiwan. *P. amboinicus* and RosA were kindly provided by Dr. Chi-Huey Wong (Academia Sinica, Taiwan). RANKL and M-CSF were purchased from Peprotech (London, UK). Anti-NF-κB p65, anti-IκBα, anti-p38, anti-ERK, anti-phospho-p38, and anti-phospho-ERK antibodies were obtained from Cell Signaling Technology (Danvers, MA, USA). Anti-ß-actin was from Sigma Chemical Co. Anti-NFATc1 was purchased from Santa Cruz Biotechnology (Santa Cruz, CA, USA). All other reagents were purchased from Sigma Chemical Co. or Wako Pure Chemical Industries Ltd.

Purification of rosmarinic acid from P. amboinicus. RosA was purified from crude *P. amboinicus* extract as described[21]. *P. amboinicus* crude leaf juice was centrifuged at 10,000 ×g for 30 min, and the supernatant was filtered. The filtrate was lyophilized to yield a dry powder. Then the powder was separated into 16 fractions by RPC18-HPLC. The dry powder fraction no. 10 was reconstituted in 50% acetonitrile-water mixture with 0.1% trifluoroacetic acid and purified by RPC18-HPLC. The fraction was monitored at 214 nm. A linear gradient from 90% solvent A (98% water, 2% acetonitrile, 0.1% trifluoroacetic acid) to 20% solvent B (90% acetonitrile, 10% water, 0.1% trifluoroacetic acid) in 30 min was used to purify RosA. The column was reequilibrated with 90% solvent A for 20 min prior to each injection. Peaks were further collected by a model CHF122SB Advantec fraction collector. RosA was found in the peak with TR = 17.5 min as a single compound identified by mass spectrometry. The structure of RosA was identified by NMR spectroscopy (Figure 1). It was determined that 1 g of *P. amboinicus* crude dry powder can yield 8.9 mg of RosA.

MTT assay. Cells (1×10^4 cells/well) were seeded in a 96-well plate with medium supplemented with 10% fetal bovine serum (FBS) and treated with various concentrations of *P. amboinicus* and RosA for 24 h, and then washed 3 times with phosphate-buffered saline (PBS) and treated with medium containing 500 μg/ml 3-(4,5-dimethylthiazol-2-yl)-2,5-diphenyltetrazolium bromide (MTT) for 30 min at 37°C. Cells were then washed with PBS and solubilized in 100 μl DMSO. The intracellular purple formazan concentrations were determined at 550 nm in an ELISA plate reader.

Bone marrow macrophage culture and osteoclast differentiation. Bone marrow cells from DBA/1J mice were obtained for osteoclast progenitor cell preparation. Bone marrow cells were isolated from tibias and femurs of 8-week-old male mice by flushing the bone marrow cavity with PBS. The

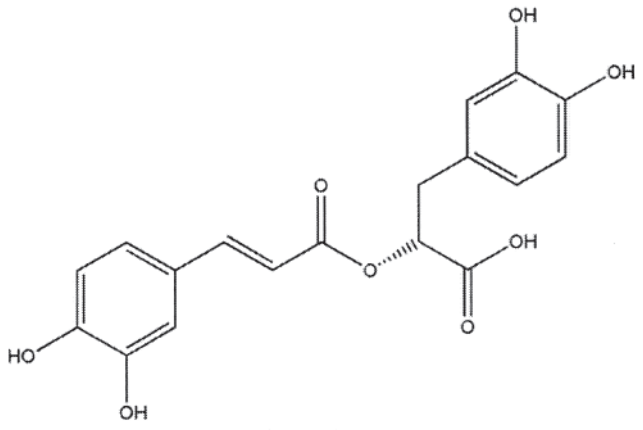

Figure 1. The chemical structure of RosA.

cells were centrifuged at 1000 ×g for 10 min and exposed to 5 ml of hypotonic ACK buffer [0.15 mM NH_4Cl, 1 mM KCO_3, and 0.1 mM EDTA (pH 7.4)] at room temperature for 5 min to remove the red blood cells. They were incubated with α-MEM (Gibco BRL) containing penicillin (100 U/ml), streptomycin (100 μg/ml), and 10% heat-inactivated FBS for 12 h to separate the floating and adherent cells. The floating cells were collected, suspended in α-MEM, counted, seeded onto a 96-well plate (4×10^4 cells/well), and cultured in α-MEM in the presence of 30 ng/ml M-CSF for 3 days to form macrophage-like osteoclast precursor cells. After the floating cells, including the lymphocytes, were removed by aspiration, the adherent osteoclast precursors were cocultured with activated lymphocytes in the presence of 30 ng/ml M-CSF and 100 ng/ml RANKL as well as *P. amboinicus* and RosA for 5 days to generate osteoclasts. On Day 3, the medium was replaced with fresh medium containing M-CSF, RANKL, *P. amboinicus*, and RosA.

Cell culture of murine RAW264.7. The murine monocyte/macrophage cell line RAW264.7 was cultured with Dulbecco modified Eagle's medium (Gibco BRL) containing 10% heat-inactivated FBS, penicillin (100 U/ml), and streptomycin (100 μg/ml). All cells were grown in a humidified atmosphere containing 5% CO_2 at 37°C. To induce osteoclast differentiation, RAW264.7 cells were suspended in α-MEM containing 10% FBS, 2 mM L-glutamate, 100 U/ml penicillin, and 100 μg/ml streptomycin; seeded 10^4 cells/dish in a 96-well plate; and cultured with 100 ng/ml soluble RANKL for 5 days. The medium was changed on Day 3.

Tartrate-resistant acid phosphatase (TRAP) staining. Cells were washed with PBS and fixed with 3.7% formaldehyde for 30 min. After washing with PBS, cells were incubated at 37°C in a humid and light-protected incubator for 1 h in the reaction mixture of the Leukocyte Acid Phosphatase Assay kit (Cat. 387, Sigma), as directed by the manufacturer. Cells were washed 3 times with distilled water and TRAP-positive multinucleated cells containing 5 or more nuclei were counted under a light microscope and photographed.

Pit formation assay. To assess the effect of *P. amboinicus* and RosA on RANKL-induced bone resorption, BMM were seeded onto 20 mm^2 dentine slices (Cat. 3988, Corning) in 24-well plates, 10^5 cells per well. All cultures were incubated in triplicate, and cells were replenished every 3 days with fresh medium containing test chemicals. Then the dentine slice was treated with 1 N NH_4OH with sonication for 5 min. Resorption pits on the dentine slices were visualized by staining with Mayer's hematoxylin solution (Sigma). The ratios of the resorbed area to the total area were measured in 4 optical fields on a slice using US National Institutes of Health Image software at 100-fold magnification.

Reverse transcription-polymerase chain reaction (RT-PCR) analysis. Total RNA was isolated from cultured cells with TRIzol reagent (Invitrogen) and reverse-transcribed using SuperScript II reverse transcriptase (Invitrogen). PCR was performed with mouse-specific primers (Table 1). Thermal cycling parameters were 95°C for 5 min, followed by 25~30 cycles for 30 s at 95°C, 30 s at 61°C, and 1 min at 72°C, and 10 min at 72°C for the final elongation. The number of cycles for each gene was determined to be in the range of linear amplification through an optimization experiment. PCR products were separated on 1.5% agarose gels, visualized by ethidium bromide staining, and analyzed densitometrically using a Phosphoimager and Quantity One software. The optical densities for each gene were normalized to the corresponding values for glyceraldehyde-3-phosphate dehydrogenase (GAPDH).

Immunoblotting analysis. Nuclear extracts were prepared according to the method of Andrews and Faller. In brief, BMM treated with or without RosA in the absence or presence of 100 ng/ml RANKL were harvested, washed with PBS, suspended in 400 μl of buffer A (10 mM HEPES-KOH, pH 7.8, 10 mM KCl, 2 mM $MgCl_2$, 0.1 mM EDTA, 1 mM DTT, 0.1 mM PMSF), and incubated on ice for 15 min. Nuclei were pelleted by centrifugation for 5 min at 14,000 rpm, and the supernatant was collected as the cytoplasmic fraction. The nuclei were resuspended in 40 μl of buffer C [50 mM HEPES-KOH, pH 7.8, 50 mM KCl, 300 mM NaCl, 0.1 mM EDTA, 1 mM DTT, 0.1 mM PMSF, 25% glycerol (vol/vol)], incubated on ice for 20 min, and centrifuged for 5 min at 14,000 rpm at 4°C. The supernatant was used as the nuclear extract. Equivalent amounts of protein were loaded for sodium dodecyl sulfate-polyacrylamide gel electrophoresis (SDS-PAGE), and immunoblotting was performed using specific antibodies for p38, phospho-p38, ERK, phospho-ERK, IκBα, NF-κB p65, NFATc1, and ß-actin.

Table 1. PCR was performed with mouse-specific primers.

Genes	Nucleotide Sequences
c-Fos	5'-GGT TTC AAC GCC GAC TAC GAG-3' (forward)
	5'-CTG ACA CGG TCT TCA CCA TTC C-3' (reverse)
NFATc1	5'-CCC TGA CCA CCG ATA GCA CTC T-3' (forward)
	5'-GGC TGC CTT CCG TCT CAT AGT G-3'(reverse)
OSCAR	5'-TCA TCT GCT TGG GCA TCA TAG T-3' (forward)
	5'-AAT AAG GCA CAG GAA GGA AAT AGA G-3' (reverse)
TRAP	5'-ACG GCT ACT TGC GGT TTC ACT A-3' (forward)
	5'-GTG TGG GCA TAC TTC TTT CCT GT-3' (reverse)
DC-STAMP	5'-CCG CTG TGG ACT ATC TGC TGT A-3' (forward)
	5'-TTC CCG TCA GCC TCT CTC AAT-3' (reverse)
ß3 integrin	5'-GTG TTT ACC ACG GAT GCC AAG A-3' (forward)
	5'-GGT GGC ATT GAA GGA CAG TGA C-3' (reverse)
GAPDH	5'-GTG AGG CCG GTG CTG AGT ATG T-3' (forward)
	5'-ACA GTC TTC TGG GTG GCA GTG AT-3' (reverse)

NFATc1 immunofluorescent staining. BMM were seeded onto glass coverslips and then incubated with 30 ng/ml M-CSF and 100 ng/ml RANKL in the presence or absence of RosA. The distribution of NFATc1 protein 24 h after stimulation was assessed according to published protocols[22]. Coverslips were removed, washed in PBS, fixed in 4% paraformaldehyde, permeabilized with 0.1% Triton X-100, incubated with 5% bovine serum albumin, and incubated overnight with a specific anti-NFATc1 monoclonal antibody (1:50; Santa Cruz Biotechnology). Cells were washed in PBS, incubated 2 h with FITC-conjugated goat anti-mouse IgG (Jackson ImmunoResearch Laboratories, West Grove, PA, USA). After the immunostaining procedures, cells were nuclear-stained with DAPI (Sigma). Fluorescence was visualized using a Leica fluorescence microscope. The percentage of cells displaying nuclear staining was then quantified; 100 cells per group were measured from 3 separate coverslips per group.

CIA mouse experiments. DBA/1J mice, 6–8 weeks old, were housed in polycarbonate cages and fed with standard mouse chow and water ad libitum. Mice were maintained under climate-controlled conditions under 12 h light–dark cycle. Twelve mice were divided into 3 groups as follows: (1) CIA; (2) CIA plus vehicle; (3) CIA plus *P. amboinicus* (375 mg/kg).

Induction of CIA and P. amboinicus treatment. CIA was induced as described with minor modifications[23]. Briefly, male DBA/1J mice were given an intradermal injection of 100 μg bovine type II collagen emulsified in complete Freund's adjuvant (1:1, wt/vol; Chondrex, Redmond, WA, USA) into the middle region of the tail. Two weeks later, mice were given a booster intradermal injection of 100 μg bovine type II collagen emulsified in incomplete Freund's adjuvant (1:1, vol/vol; Chondrex) into the base of the tail. *P. amboinicus* was dissolved in saline. After the second immunization, development of rheumatic symptoms was observed approximately on Day 22 and mice were administered test compounds by gavages after symptoms were first observed for 4 weeks. Mice were sacrificed under CO_2 euthanasia on Day 50 and hind leg joints were collected for histopathological assessments.

Determination of murine IL-1ß and TNF-α protein levels. For quantitative analysis of IL-1ß and TNF-α protein expression in serum, ELISA kits (R&D Systems, Minneapolis, MN, USA) were used according to the manufacturer's instructions. Murine IL-1ß and TNF-α protein levels were measured in mouse serum and the reaction was quantified in an ELISA microplate reader.

Clinical assessments of arthritic index and paw thickness in CIA mice. A blinded independent observer with no knowledge of the treatment protocol performed evaluation of joint inflammation. The severity of arthritis in each footpad was quantified daily by a clinical score measurement. The level of arthritic inflammation of each paw was graded 0 to 4 according to Campo, *et al*[24]. The maximum arthritic index of 4 paws was summed for each animal and ranged from 0 to 16 (0 = no disease; 16 = highest possible score). The degree of paw swelling was measured using a caliper. The increased thickness of paws was compared with normal mice without collagen immunization.

Histopathological assessment of arthritis. Sections were evaluated blindly as described[25]. Ankle joints were stored in 10% neutral buffered formalin for at least 24 h prior to placement in decalcifier. After 1 day of decalcification, the digits were trimmed and the ankle joint was transected in the longitudinal plane to give approximately equal halves. These were processed for paraffin embedding, sectioned, and stained with hematoxylin and eosin for inflammation and bone erosion. Multiple sections were prepared to ensure that the distal tibia with both cortices was present and that abundant distal tibial medullary space was available for evaluation. Bone destruction was graded on a scale of 0–5, ranging from no damage to complete loss of the bone structure. Ankles of CIA mice were also scored 0–5 for inflammation (0 = normal; 1 = minimal infiltration of inflammatory cells in periarticular tissue; 2 = mild infiltration; 3 = moderate infiltration, with moderate edema; 4 = marked infiltration, with marked edema; and 5 = severe infiltration, with severe edema). Cartilage damage was not scored in the adjuvant arthritis model because we have found this generally to be a minor feature not reliable for evaluation of potential treatment effects.

Statistical analysis. Data were expressed as means ± SD. Statistical analyses were performed by a paired 2-tailed Student t-test assuming equal variances. Values of $p < 0.05$ were considered to indicate statistical significance.

RESULTS

Effects of P. amboinicus and RosA on RANKL-induced osteoclast differentiation. We screened for natural compounds that could potentially inhibit osteoclastogenesis by evaluating the activity of TRAP, a specific marker of osteoclast differentiation, using osteoclast precursor cell line RAW264.7. RosA decreased the number of multinucleated osteoclasts in a dose-dependent manner (Figure 2C, 2D). The effects of *P. amboinicus* and RosA on osteoclastogenesis were further confirmed by using primary BMM. Murine BMM were formed from bone marrow cells within 3 days in response to M-CSF (30 ng/ml). BMM were cultured in the presence of M-CSF (30 ng/ml) and RANKL (100 ng/ml) together with or without various concentrations of *P. amboinicus* or RosA for 5 days. Both *P. amboinicus* and RosA inhibited osteoclast formation in a concentration-dependent manner when added throughout the entire culture period (Figure 2A, 2E). The IC_{50} values of *P. amboinicus* and RosA for TRAP-positive multinucleated osteoclast formation were 50 μg/ml and 40 μM, respectively (Figure 2B, 2F). RosA reduced the number of TRAP-positive multinucleated cells generated with 49% ± 4.7% and 84.1% ± 1.9% inhibition at 40 μM and 80 μM concentrations, respectively (Figure 2F). RosA 80 μM completely suppressed multinucleated osteoclast formation in RAW264.7 cells (Figure 2D). To examine the effect of *P. amboinicus* and RosA on cell growth, we treated cells with various concentrations of *P. amboinicus* or RosA for 24 h and measured cell growth by an MTT assay. *P. amboinicus* and RosA did not affect the cell growth rate of BMM and RAW264.7 (Figure 3A, 3B), sustaining substantial viability even when used at concentrations that significantly inhibited osteoclast formation.

Effects of RosA on NFATc1-regulated gene expression during RANKL-induced osteoclast development. Osteoclast differentiation is associated with upregulation of specific genes in response to RANKL and RANK binding. The *c-fos* and *NFATc1* genes have been reported to play a pivotal role in osteoclast differentiation, and NFATc1 regulates OSCAR expression[26]. As well, *DC-STAMP* is essential for cell–cell fusion during RANKL-mediated osteoclastogenesis[27,28]. *ß3 integrin* is involved in osteoclast differentiation[29]. Therefore, we examined the effects of RosA on the RANKL-induced regulation of *c-fos* and *NFATc1* expression and assessed whether there were any effects on *TRAP*, *OSCAR*, *DC-STAMP*, and *ß3 integrin* expression. BMM were pretreated with or without RosA and further stimulated with RANKL (100 ng/ml) in the presence of M-CSF (30 ng/ml) at various timepoints. Results revealed that *c-fos* and *NFATc1* mRNA levels were increased in response to RANKL, but expression of both *c-fos* and *NFATc1* was significantly inhibited by RosA. *TRAP*, *OSCAR*, *DC-STAMP*, and *ß3 integrin* mRNA expression was also significantly inhibited by RosA in a concentration-dependent manner (Figure 4). This raises the possibility that RosA may inhibit osteoclast differentiation through inhibition of RANKL-induced *c-fos* and *NFATc1* expression.

Effects of RosA on RANKL-induced MAPK activation in osteoclasts. Reports have indicated that RANKL induces the activation of 3 well known MAPK (ERK, JNK, and p38) in osteoclast precursor cells[30] and RAW264.7 cells[31]. These kinases (especially ERK and JNK) also participate in c-Fos and c-Jun activation in osteoclast precursors[32,33]. Based on the findings that RosA suppressed RANKL-induced *c-fos* mRNA expression, we next investigated whether MAPK were involved in the inhibition of osteoclastogenesis by RosA in BMM. RANKL (100 ng/ml) markedly activated p38 and ERK phosphorylation measured at the early timepoint of 30 min. Results indicated that RANKL-induced phosphorylation was inhibited by RosA in a concentration-dependent manner (Figure 5A).

Effect of RosA on RANKL-activated IκB/NF-κB. Activation of NF-κB is important in the activation and survival of mature osteoclasts, as well as osteoclastogenesis[34]. Recent studies have suggested that NF-κB is another upstream transcription factor modulating NFATc1 expression[35]. Activity of NF-κB is regulated by its inhibitor, IκB, which forms a complex with NF-κB in the cytoplasm. IκB degradation through an ubiquitin/proteasome pathway unmasks the nuclear localization signal motif of NF-κB, which allows the transcription factor to translocate from the cytoplasm into the nucleus. To investigate the molecular mechanism of

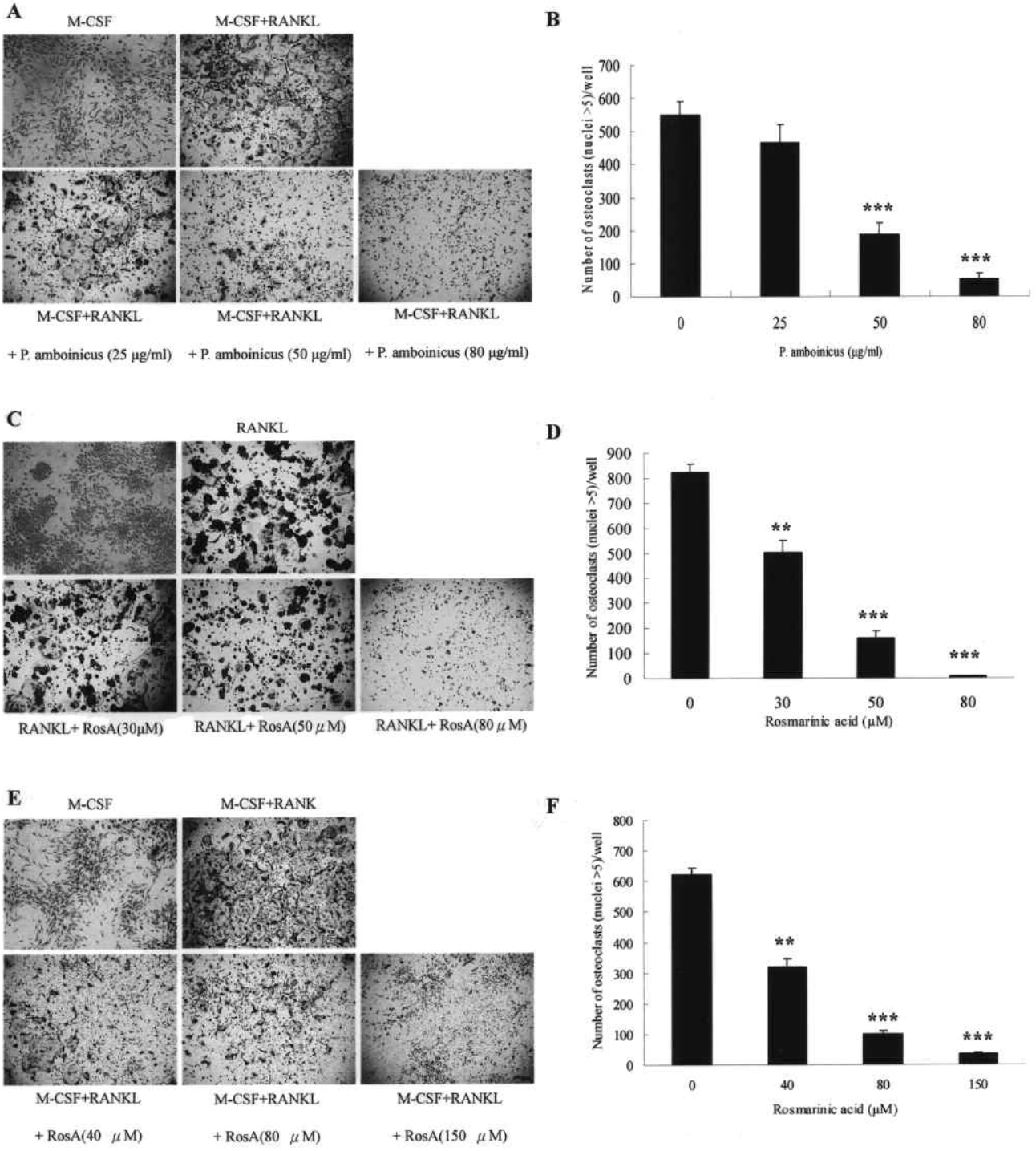

Figure 2. Effects of *P. amboinicus* and RosA on RANKL-induced osteoclast differentiation of murine bone marrow-derived macrophages (BMM) and RAW264.7. A, B: BMM treated with M-CSF (30 ng/ml) were cultured with or without *P. amboinicus* in the presence of RANKL (100 ng/ml) for 5 days. C, D: RAW264.7 cells were cultured with or without RosA in the presence of RANKL (100 ng/ml) for 5 days. E, F: BMM treated with M-CSF (30 ng/ml) were cultured with or without RosA in the presence of RANKL (100 ng/ml) for 5 days. After the culture, the cells were fixed and stained for TRAP, and TRAP-positive multinucleated cells containing more than 5 nuclei were counted as multinucleated osteoclasts. The data represent means ± SD of more than 3 cultures. $^{**}p < 0.01$, $^{***}p < 0.005$, significantly different from values after treatment with RANKL alone.

RosA-mediated inhibition of osteoclast differentiation, we examined the effect of RosA on changes in IκB and NF-κB after RANKL stimulation. As shown in Figure 5C, RosA reduced RANKL-induced IκB degradation within 30 min in a concentration-dependent manner. Further, nuclear translocation of NF-κB p65 was investigated. Results showed that

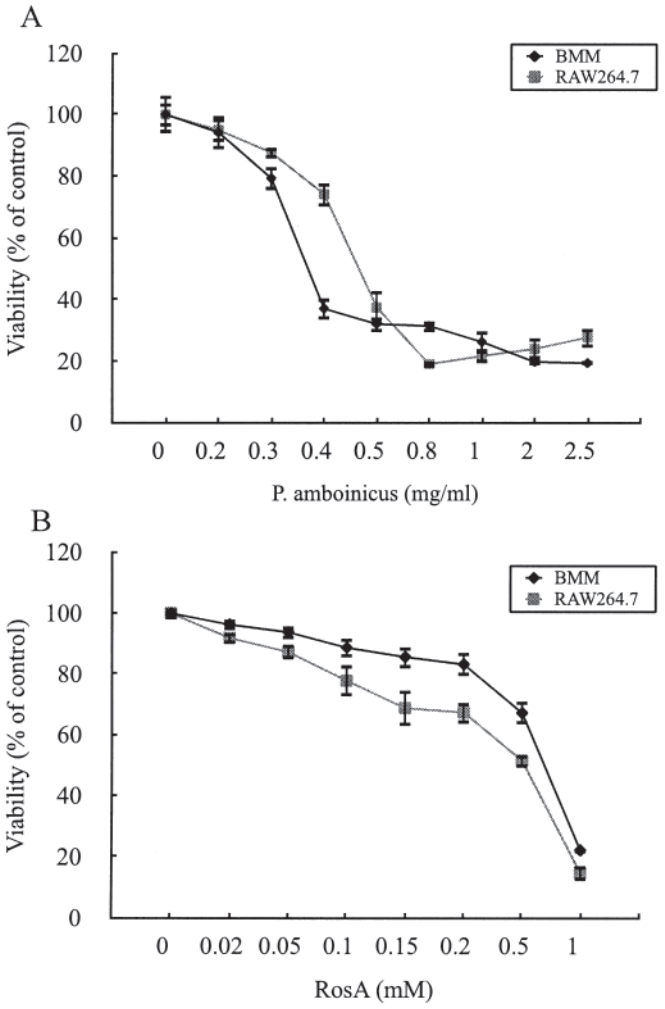

Figure 3. Effect of *P. amboinicus* (A) and RosA (B) on cytotoxicity. Murine bone marrow-derived macrophages (BMM) and RAW264.7 cells were seeded onto 96-well plates. Cells were cultured 24 h with the indicated concentrations of *P. amboinicus* and RosA. After 24 h, MTT solution (500 μg/ml) was added to each well. The optical density was read at 550 nm in an ELISA plate reader after 30 min incubation. Cell viability was determined relative to the control. Data represent means ± SD of more than 3 cultures.

RosA blocked IκB degradation and concomitantly suppressed the subsequent nuclear translocation of NF-κB p65 (Figure 5B).

Effects of RosA on RANKL-induced nuclear translocation and expression of NFATc1. Binding of RANKL to RANK activates several transcription factors responsible for promoting osteoclastic gene expression. These are not all activated within the same timeframe: early-response factors, such as NF-κB, are activated before late-response factors such as NFATc1[36]. NFATc1 is one of the key transcription factors involved in osteoclast differentiation by RANKL[37]. In the inactive state, NFATc1 is retained in the cytoplasm. When being activated, NFATc1 is translocated from the cytoplasm into the nucleus. Therefore, we examined the effect of RosA on the nuclear translocation of NFATc1 in RANKL-activated BMM by immunofluorescent staining. As shown in Figure 6A, the majority of NFATc1 was located primarily in the cytoplasm. Upon RANKL stimulation, nuclear accumulation of NFATc1 was markedly increased by RANKL stimulation for 24 h compared with the levels in cells without RANKL treatment. This elevated level of nuclear NFATc1 was reduced by RosA in a concentration-dependent manner. To further confirm whether RosA suppressed NFATc1 nuclear translocation at the protein level, we performed Western blotting to analyze NFATc1 in nuclear extracts and cytoplasmic extracts. The data showed that NFATc1 in whole-cell extracts and nuclear extracts increased dramatically after 24 h treatment by RANKL. However, treatment of RosA inhibited NFATc1 expression and its nuclear translocation (Figure 6B), suggesting that RosA suppressed RANKL-induced NFATc1 nuclear translocation and activation during osteoclastogenesis in BMM.

Effects of P. amboinicus and RosA on bone resorption in cell cultures. To examine the effects of RosA on osteoclastic bone resorption, resorption pit formation was assessed. BMM were plated onto dentine slices, and then differentiated into osteoclasts by RANKL treatment for 5 days in the absence or presence of *P. amboinicus* or RosA. After culture for 5 days, many resorption pits were formed on the bone slices. RANKL-evoked bone resorption was dose-dependently diminished by concurrent addition of *P. amboinicus* (Figure 7A) or RosA (Figure 7B) in BMM. These results indicated that both *P. amboinicus* and RosA prevented osteoclastic bone resorption by inhibiting osteoclastogenesis.

Effects of P. amboinicus treatment on arthritis scores and paw swelling. Arthritis developed roughly 3 weeks after the primary immunization with type II collagen. *P. amboinicus* significantly reduced the mean arthritis scores (Figure 8A) and paw swelling (Figure 8B) compared with the vehicle group.

Effects of P. amboinicus treatment on histological findings. After receiving *P. amboinicus* (375 mg/kg) by gavage for 4 consecutive weeks, mice were sacrificed to assess the effects of *P. amboinicus* on synovial inflammation and bone erosion by H&E staining and ELISA. The *P. amboinicus*-treated mice had much less infiltration of inflammatory cells, synovial hyperplasia, and articular bone destruction in inflamed joints than the vehicle-treated mice. Our data showed that *P. amboinicus* markedly reduced CIA-evoked synovial inflammation and bone destruction (Figure 9A). Studies have shown that regulation of the production of proinflammatory cytokines during CIA is critical in the control of synovial inflammation and tissue destruction[38,39]. To elucidate how *P. amboinicus* ameliorates CIA, we investigated the effects of *P. amboinicus* on the levels of TNF-α and IL-1ß in serum. Blood was withdrawn from the heart on Day 50, and the levels of the 2 cytokines were measured by ELISA. Consistent with the joint-swelling result, marked

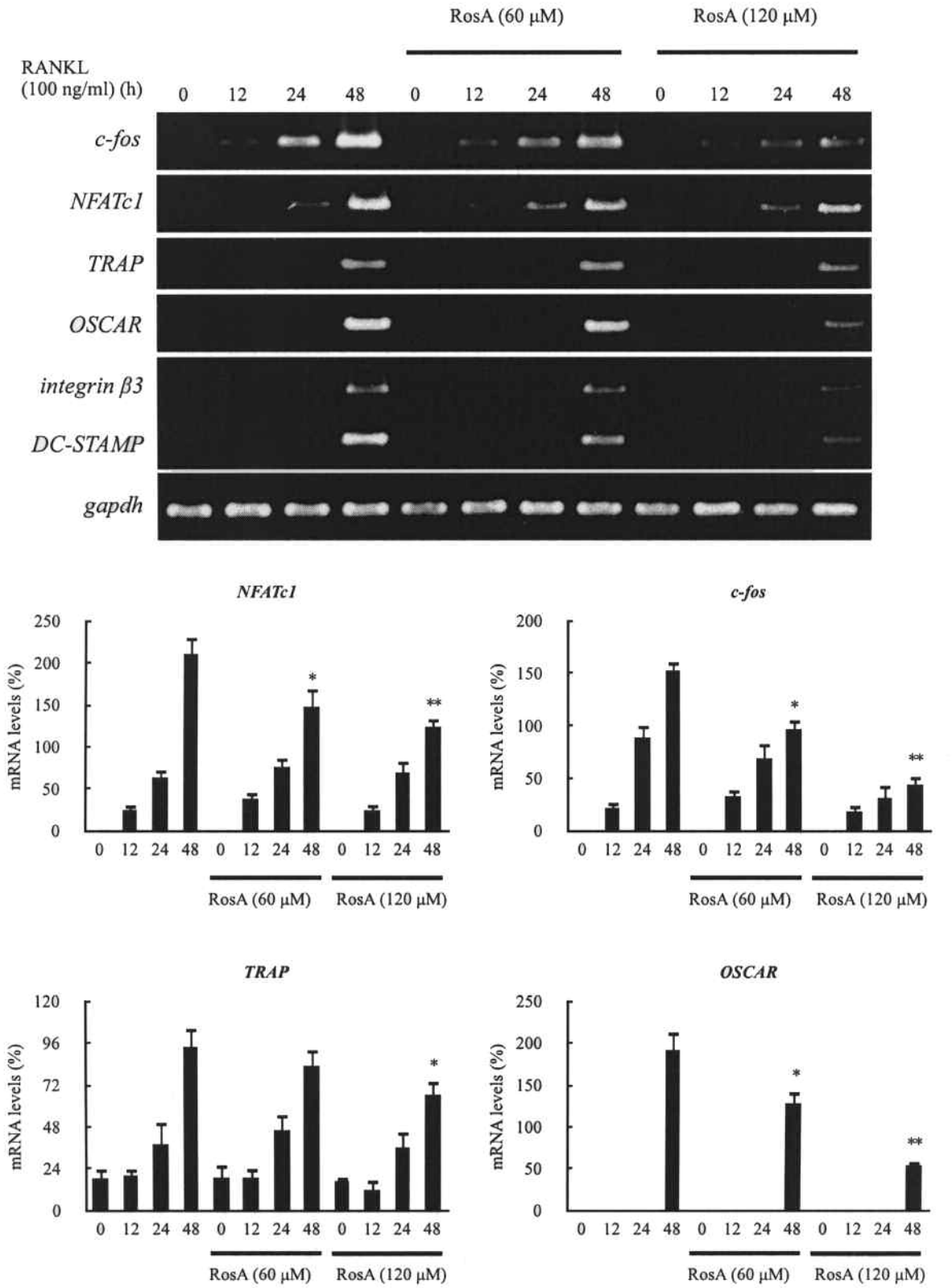

Figure 4. Effects of RosA on NFATc1-mediated mRNA expression. Murine bone marrow-derived macrophages (BMM) were pretreated with or without RosA for 1 h and with RANKL (100 ng/ml) for the indicated time periods. Total RNA was isolated with TRIzol, and 1 μg of total RNA was used to transcribe cDNA. cDNA was used as a template for PCR with mouse-specific primers. Data represent means ± SD of more than 3 cultures. *$p < 0.05$, **$p < 0.01$, significantly different from values after treatment with RANKL alone.

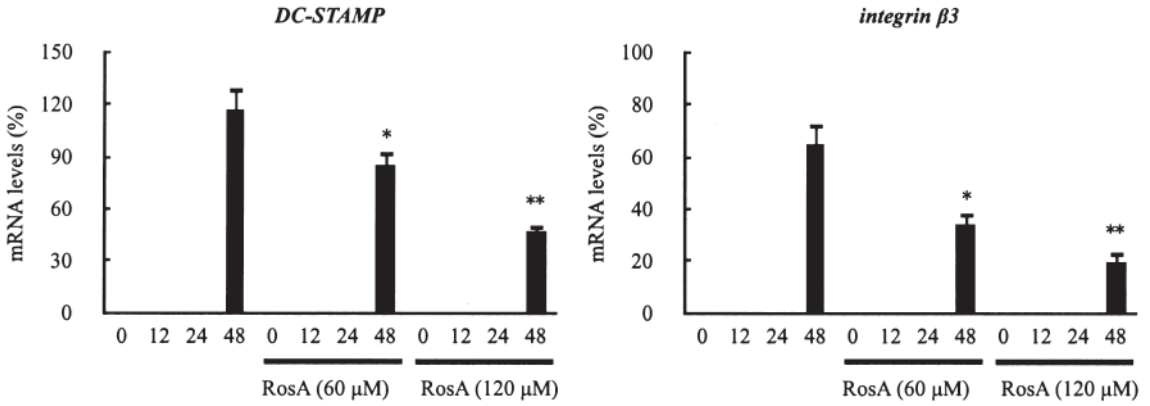

Figure 4. Continued.

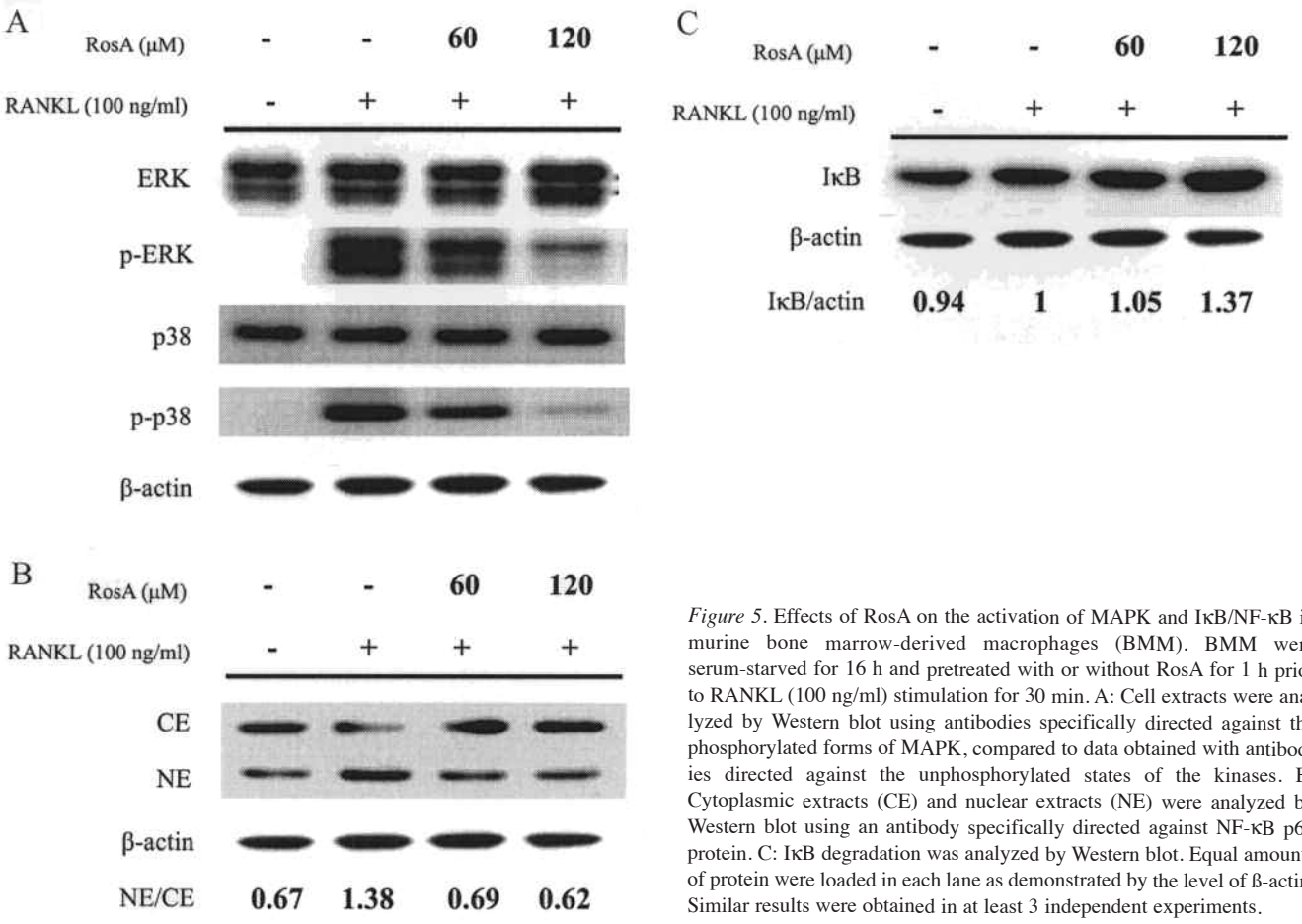

Figure 5. Effects of RosA on the activation of MAPK and IκB/NF-κB in murine bone marrow-derived macrophages (BMM). BMM were serum-starved for 16 h and pretreated with or without RosA for 1 h prior to RANKL (100 ng/ml) stimulation for 30 min. A: Cell extracts were analyzed by Western blot using antibodies specifically directed against the phosphorylated forms of MAPK, compared to data obtained with antibodies directed against the unphosphorylated states of the kinases. B: Cytoplasmic extracts (CE) and nuclear extracts (NE) were analyzed by Western blot using an antibody specifically directed against NF-κB p65 protein. C: IκB degradation was analyzed by Western blot. Equal amounts of protein were loaded in each lane as demonstrated by the level of ß-actin. Similar results were obtained in at least 3 independent experiments.

decreases in the levels of TNF-α and IL-1ß were observed in the mice treated with *P. amboinicus* compared with the control mice (Figure 9B). These results suggested that *P. amboinicus* inhibited the production of proinflammatory cytokines in the CIA mice.

DISCUSSION

The major remedies currently used in osteoporosis treatment primarily include estrogen replacement therapy along with bisphosphonates (e.g., alendronate, risedronate), selective estrogen receptor modulators, and calcitonin. However,

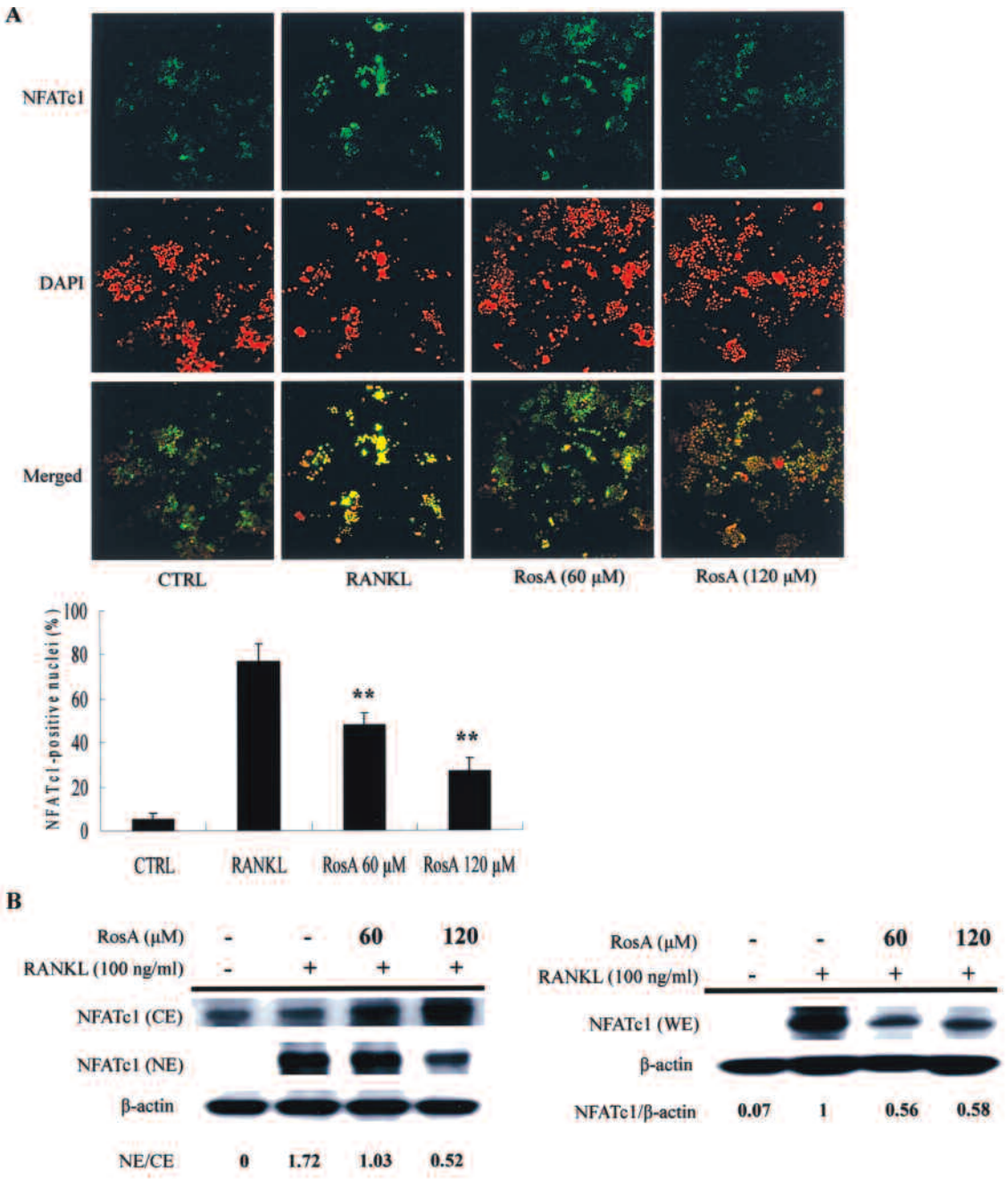

Figure 6. Effects of RosA on RANKL-induced nuclear translocation of NFATc1. A: Immunofluorescent analysis. Murine bone marrow-derived macrophages (BMM) were cultured with or without RANKL (100 ng/ml) in the presence of M-CSF (30 ng/ml). RosA was added to some of the cultures treated with RANKL. After 24 h, the cells were stained with anti-NFATc1 antibody (green) and DAPI (nuclear staining, red) (upper panels). The nuclear localization of NFATc1 was confirmed in merged images of BMM treated with RANKL (yellow). NFATc1-positive nuclei were counted in BMM (lower panel). Data represent the means ± SD of more than 3 cultures. **p < 0.01, significantly different from the culture treated with RANKL alone. B: Western blot analysis. BMM were serum-starved for 16 h and then incubated with RANKL (100 ng/ml) for 24 h in the absence or presence of RosA 1 h prior to RANKL. Whole-cell extracts (WE), cytoplasmic extracts (CE), and nuclear extracts (NE) were analyzed by Western blot using antibody specifically directed against NFATc1 protein. Equal amounts of protein were loaded in each lane as demonstrated by the level of ß-actin.

these therapies are associated with undesired effects such as breast cancer, endometritis, thromboembolism, hypercalcemia, gastrointestinal problems, and hypertension[40,41,42,43,44,45]. Although a panel of drugs has been developed for the treatment of RA, therapies for RA are not satisfied with these marketed drugs.

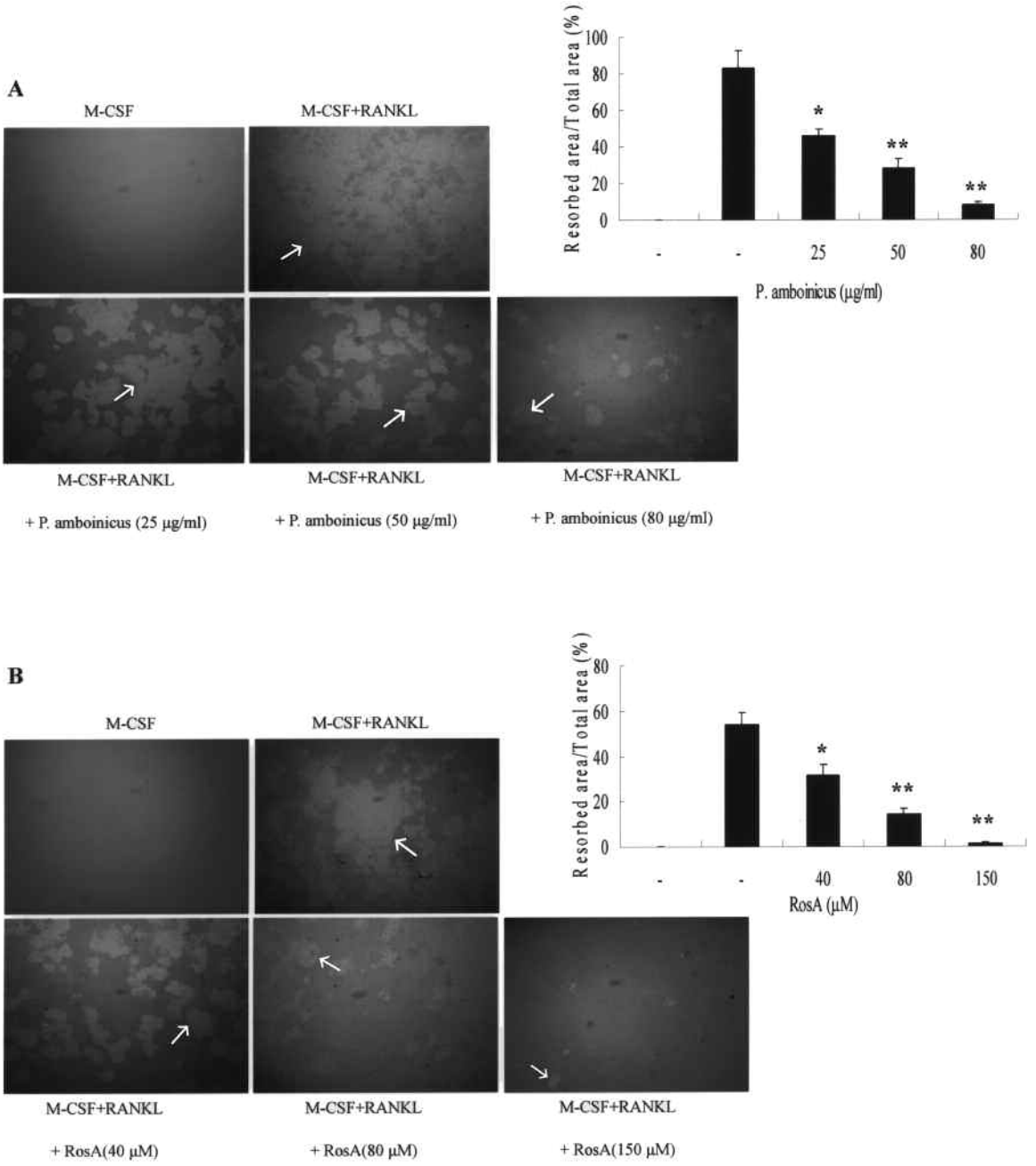

Figure 7. Effects of *P. amboinicus* and RosA on resorption pit formation. Murine bone marrow-derived macrophages (BMM) were cultured on bone slices with various concentrations of *P. amboinicus* (A) or RosA (B) in the presence of RANKL (100 ng/ml). After culturing for 5 days, the dentine slices were recovered for Mayer's hematoxylin staining to visualize resorption pits; arrows indicate pit area. Percentages of the resorbed area were determined using US NIH Image software. Data represent the means ± SD of more than 4 slices. *$p < 0.05$ and **$p < 0.01$, significantly different from values after treatment with RANKL alone.

P. amboinicus, belonging to the *Lamiaceae* family, is a perennial with a 3- to 10-year lifespan; it is distributed in tropical Africa, Asia, and Australia. It is used as a food, additive, fodder, and especially as a medicine in treating a wide range of diseases[46]. We examined the effects of *P. amboinicus* on osteoclast differentiation and identified the active ingredient. The crude extract of *P. amboinicus* was further separated into 16 fractions using HPLC. After the crude extract was fractionated, all the fractions were subjected to TRAP activity assay to determine which fraction consisted of active compounds that exert an inhibitory effect on osteoclastogenesis. Our data suggested that RosA, a phytopolyphenol purified from fraction no. 10, inhibited RANKL-induced osteoclast formation as effectively as the

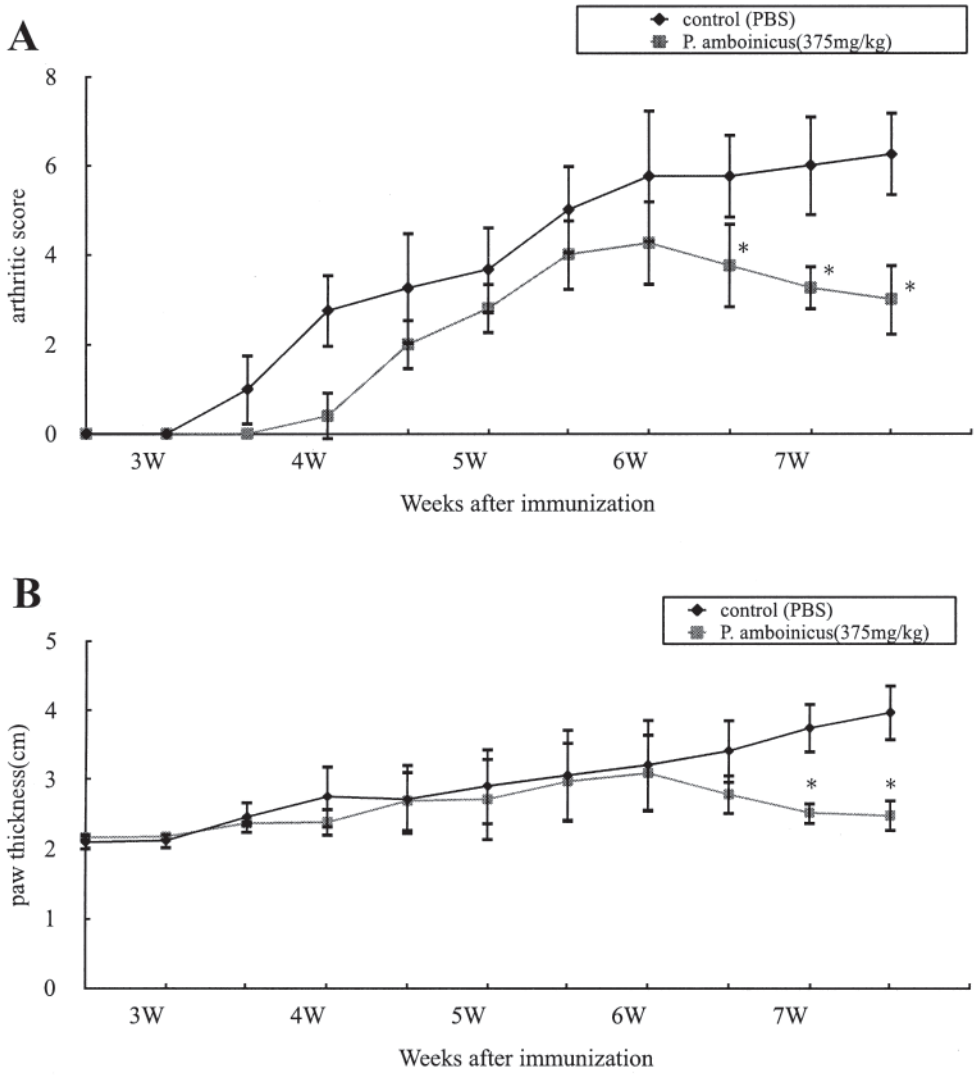

Figure 8. Effects of *P. amboinicus* on arthritis scores and paw swelling with time course in CIA mice. Mice were administered placebo and *P. amboinicus* by gavage 3 times a week for 4 weeks. Arthritis scores (A) and paw thickness (B) were measured at 3-day intervals. *P. amboinicus* markedly reduced the mean arthritis scores and paw swelling. Data represent means ± SD of 4 mice. *$p < 0.05$, in comparison with relevant controls.

crude *P. amboinicus* extract did in BMM. These phenomena were not attributed to the cytotoxicity of *P. amboinicus* and RosA. Other compounds of fractions no. 8 and no. 9 showed inhibitory activities as well (data not shown).

RosA is an ester of caffeic acid and 3,4-dihydroxy-phenyllactic acid. RosA can be found in numerous plants, including species of the *Boraginaceae* and the *Lamiaceae*. Previous studies revealed that RosA has several antiinflammatory and antiallergic properties[47,48]. Youn, *et al* demonstrated that RosA suppressed synovitis in CIA mice and that it may be beneficial for treatment of RA[49]. Moreover, it has been reported that osteoclast formation is enhanced in CIA rats[50]. However, the effects of RosA on bone metabolism are not yet known.

Bone is restructured at such a high speed that approximately 10% of the total bone content is replaced every year in human adults. Osteoclast differentiation is a multistep process that involves cell proliferation, commitment, fusion, and activation. Under normal conditions, the RANKL–RANK axis appears to be essential for osteoclastogenesis[51,52]. The signaling mechanism of RANKL has been studied extensively. Binding of RANKL to RANK strongly activates the NF-κB by degradation of IκBα, allowing it to translocate into the nucleus, where it enhances transcription of target genes[53]. Our data showed that RosA suppressed the activation and nuclear translocation of NF-κB by the inhibition of IκB degradation.

In addition to NF-κB, RANKL also activates a series of

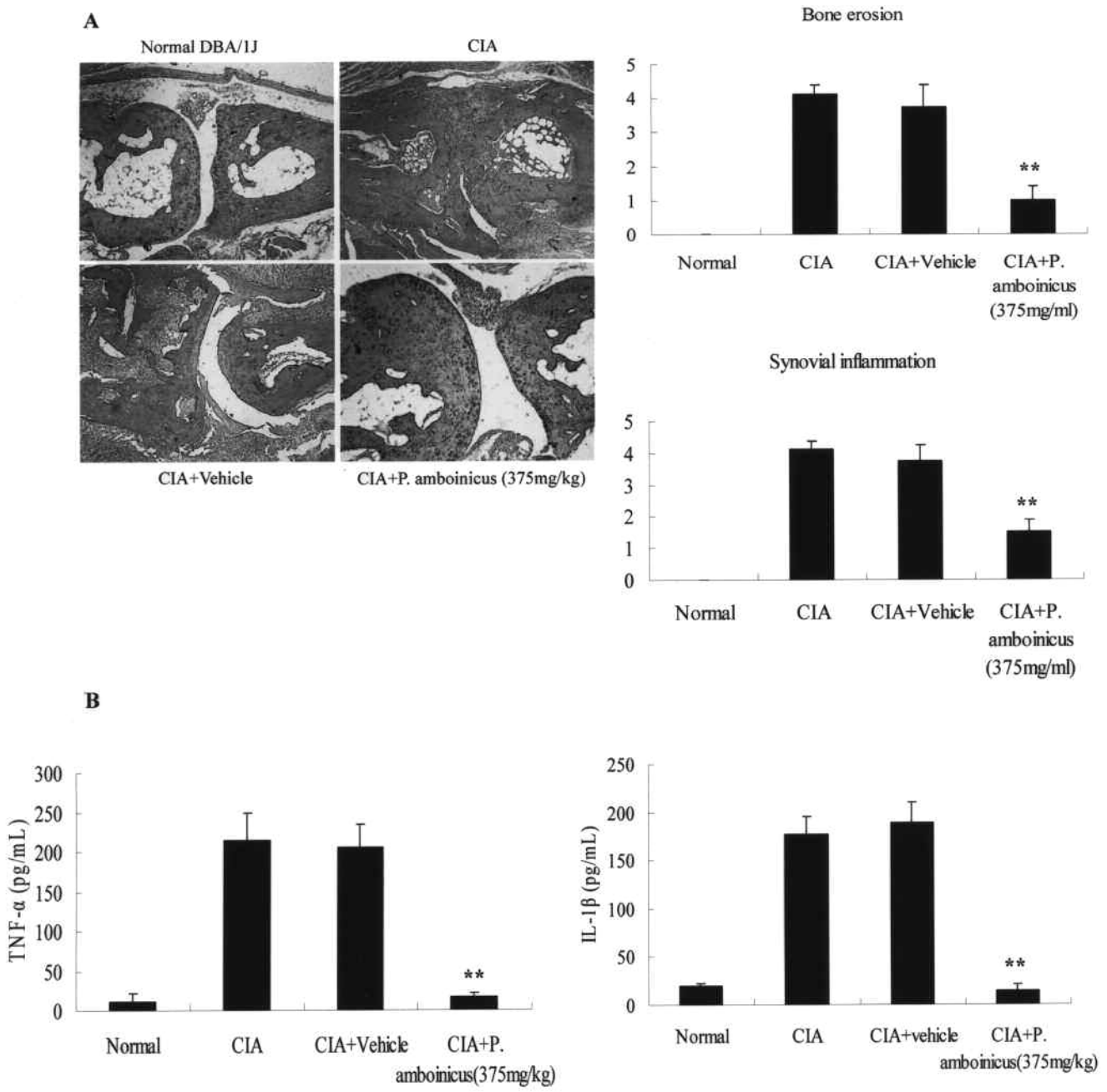

Figure 9. Effects of *P. amboinicus* on clinical evaluation and levels of serum IL-1ß and TNF-α in CIA mice. A: Representative histological sections of ankle joints were stained with H&E. Synovial inflammation and bone erosion were scored with the criteria described in Methods. There was a significant reduction in both synovial inflammation and bone erosion. B: Serum IL-1ß and TNF-α measured on Day 50. Data represent means ± SD of 4 mice. **p < 0.01, in comparison with relevant controls. A representative result of at least 3 independent experiments is shown.

major intracellular signaling transduction pathways including JNK, ERK, p38 MAPK, and transcriptional factors such as AP-1 and NFATc1. NFATc1 is a key mediator of osteoclastogenesis that autoamplifies and conducts the expression of osteoclast-specific genes including *TRAP*, *calcitonin receptor*, *OSCAR*, and *cathepsin K*[54,55]. We found that RosA decreased the phosphorylation of ERK and p38 in response to RANKL. Further, our data demonstrated that RosA also significantly suppressed not only RANKL-induced *c-fos* expression but also NFATc1 nuclear transport and further induction. It has been shown that c-Fos induces *NFATc1* expression and that c-Fos and NFATc1 cooperatively regulate osteoclastogenesis in response to RANKL stimulation. Thus, we suggested that the inhibition of RANKL-induced *c-fos* expression by RosA is a relevant factor in the suppression of downstream NFATc1 signaling pathways. As a result

of downregulation of *NFATc1* expression, the NFATc1-mediated osteoclastogenic genes such as *TRAP*, *DC-STAMP*, and *OSCAR* were also concomitantly inhibited by RosA. Considering these data together, we postulated that RosA conferred inhibitory activity on *P. amboinicus* for inhibition of osteoclastogenesis via downregulation of RANKL-induced NFATc1 expression.

RA is an autoimmune disease accompanied by hyperplasia of the cartilage lining caused by infiltration of inflammatory cells, ultimately resulting in joint damage[56]. Various cytokines are known to be involved in RA, particularly proinflammatory cytokines such as TNF-α, IL-1ß, and interferon-γ that are produced by macrophages, dendritic cells, and T cells[57]. Our data showed that *P. amboinicus* significantly ameliorated CIA and diminished TNF-α and IL-1ß production in CIA mice, consistent with a study by Chang, *et al*[20]. *P. amboinicus* suppressed the osteoclast formation in BMM and the bone erosion in CIA mice.

We provided the first evidence that RosA, an active ingredient from *P. amboinicus*, had inhibitory effects on RANKL-stimulated osteoclast differentiation and pit formation on dentine slices *in vitro*. We also provided molecular signaling pathways for this inhibition, involving MAPK and transcription factors such as NF-κB, NFATc1, and c-Fos, which act on genes involved in osteoclast differentiation. We found that RosA blocked RANKL-stimulated activation of MAPK and NF-κB/IκB signaling pathways, and subsequently suppressed NFATc1 expression. Finally, RosA inhibited osteoclast differentiation via downregulation of NFATc1-modulated gene expression. Together, our data might decipher the possible molecular mechanisms by which *P. amboinicus* mitigates CIA-evoked bone destruction, and might make *P. amboinicus* a potential novel therapy for bone disorders such as RA and osteoporosis by fine-tuning RANKL-induced osteoclast differentiation and functions.

ACKNOWLEDGMENT

We thank Dr. Chi-Huey Wong at the Academia Sinica for the kind gift of *P. amboinicus* and for assistance in purification of RosA.

REFERENCES

1. Sato K, Suematsu A, Okamoto K, Yamaguchi A, Morishita Y, Kadono Y, et al. Th17 functions as an osteoclastogenic helper T cell subset that links T cell activation and bone destruction. J Exp Med 2006;203:2673-82.
2. Nanki T, Hayashida K, El-Gabalawy HS, Suson S, Shi K, Girschick HJ, et al. Stromal cell-derived factor-1-CXC chemokine receptor 4 interactions play a central role in CD4+ T cell accumulation in rheumatoid arthritis synovium. J Immunol 2000;165:6590-8.
3. Ji H, Pettit A, Ohmura K, Ortiz-Lopez A, Duchatelle V, Degott C, et al. Critical roles for interleukin 1 and tumor necrosis factor alpha in antibody-induced arthritis. J Exp Med 2002;196:77-85.
4. Stunkard AJ, Harris JR, Pedersen NL, McClearn GE. The body-mass index of twins who have been reared apart. N Engl J Med 1990;322:1483-7.
5. Redlich K, Hayer S, Ricci R, David JP, Tohidast-Akrad M, Kollias G, et al. Osteoclasts are essential for TNF-alpha-mediated joint destruction. J Clin Invest 2002;110:1419-27.
6. Teitelbaum SL. Bone resorption by osteoclasts. Science 2000;289:1504-8.
7. Suda T, Takahashi N, Udagawa N, Jimi E, Gillespie MT, Martin TJ. Modulation of osteoclast differentiation and function by the new members of the tumor necrosis factor receptor and ligand families. Endocr Rev 1999;20:345-57.
8. Suda T, Takahashi N, Martin TJ. Modulation of osteoclast differentiation. Endocr Rev 1992;13:66-80.
9. Roodman GD. Cell biology of the osteoclast. Exp Hematol 1999;27:1229-41.
10. Chambers TJ. Regulation of the differentiation and function of osteoclasts. J Pathol 2000;192:4-13.
11. Martin TJ, Romas E, Gillespie MT. Interleukins in the control of osteoclast differentiation. Crit Rev Eukaryot Gene Expr 1998;8:107-23.
12. Darnay BG, Haridas V, Ni J, Moore PA, Aggarwal BB. Characterization of the intracellular domain of receptor activator of NF-kappa B (RANK). Interaction with tumor necrosis factor receptor-associated factors and activation of NF-kappa b and c-Jun N-terminal kinase. J Biol Chem 1998;273:20551-5.
13. Wong BR, Josien R, Lee SY, Vologodskaia M, Steinman RM, Choi Y. The TRAF family of signal transducers mediates NF-kappa B activation by the TRANCE receptor. J Biol Chem 1998; 273:28355-9.
14. Boyle WJ, Simonet WS, Lacey DL. Osteoclast differentiation and activation. Nature 2003;423:337-42.
15. Lerner UH. New molecules in the tumor necrosis factor ligand and receptor superfamilies with importance for physiological and pathological bone resorption. Crit Rev Oral Biol Med 2004; 15:64-81.
16. Teitelbaum SL, Ross FP. Genetic regulation of osteoclast development and function. Nat Rev Genet 2003;4:638-49.
17. Asagiri M, Takayanagi H. The molecular understanding of osteoclast differentiation. Bone 2007;40:251-64.
18. Vera R, Mondon JM, Pieribattesti JC. Chemical composition of the essential oil and aqueous extract of Plectranthus amboinicus. Planta Med 1993;59:182-3.
19. Chang SL, Chang YC, Yang CH, Hong HS. Allergic contact dermatitis to Plectranthus amboinicus masquerading as chronic leg ulcer. Contact Dermatitis 2005;53:356-7.
20. Chang JM, Cheng CM, Hung LM, Chung YS, Wu RY. Potential use of Plectranthus amboinicus in the treatment of rheumatoid arthritis. Evid Based Complement Alternat Med 2007 Nov 23. [Epub ahead of print]
21. Composition and methods for treating inflammation and inflammation-related disorders by Plectranthus amboinicus extract. [Internet. Accessed June 16, 2011.] Available from: http://pharma-licensing.com/public/outlicensing/view/11558/composition-and-methods-for-treating-inflammation-and-inflammation-related-disorders-by-plectranthus-amboinicus-extract
22. Evans KE, Fox SW. Interleukin-10 inhibits osteoclastogenesis by reducing NFATc1 expression and preventing its translocation to the nucleus. BMC Cell Biol 2007;8:4.
23. Park MJ, Min SY, Park KS, Cho YG, Cho ML, Jung YO, et al. Indoleamine 2,3-dioxygenase-expressing dendritic cells are involved in the generation of CD4+CD25+ regulatory T cells in Peyer's patches in an orally tolerized, collagen-induced arthritis mouse model. Arthritis Res Ther 2008;10:R11.
24. Campo GM, Avenoso A, Campo S, Ferlazzo AM, Altavilla D, Calatroni A. Efficacy of treatment with glycosaminoglycans on experimental collagen-induced arthritis in rats. Arthritis Res Ther 2003;5:R122-31.
25. Bendele A, McAbee T, Sennello G, Frazier J, Chlipala E, McCabe D. Efficacy of sustained blood levels of interleukin-1 receptor antagonist in animal models of arthritis: comparison of efficacy in

animal models with human clinical data. Arthritis Rheum 1999;42:498-506.
26. Kim K, Kim JH, Lee J, Jin HM, Lee SH, Fisher DE, et al. Nuclear factor of activated T cells c1 induces osteoclast-associated receptor gene expression during tumor necrosis factor-related activation-induced cytokine-mediated osteoclastogenesis. J Biol Chem 2005;280:35209-16.
27. Kukita T, Wada N, Kukita A, Kakimoto T, Sandra F, Toh K, et al. RANKL-induced DC-STAMP is essential for osteoclastogenesis. J Exp Med 2004;200:941-6.
28. Yagi M, Miyamoto T, Sawatani Y, Iwamoto K, Hosogane N, Fujita N, et al. DC-STAMP is essential for cell-cell fusion in osteoclasts and foreign body giant cells. J Exp Med 2005;202:345-51.
29. Zou W, Kitaura H, Reeve J, Long F, Tybulewicz VL, Shattil SJ, et al. Syk, c-Src, the alpha v beta 3 integrin, and ITAM immunoreceptors, in concert, regulate osteoclastic bone resorption. J Cell Biol 2007;176:877-88.
30. Lee SE, Woo KM, Kim SY, Kim HM, Kwack K, Lee ZH, et al. The phosphatidylinositol 3-kinase, p38, and extracellular signal-regulated kinase pathways are involved in osteoclast differentiation. Bone 2002;30:71-7.
31. Mozar A, Haren N, Chasseraud M, Louvet L, Maziere C, Wattel A, et al. High extracellular inorganic phosphate concentration inhibits RANK-RANKL signaling in osteoclast-like cells. J Cell Physiol 2008;215:47-54.
32. Grigoriadis AE, Wang ZQ, Cecchini MG, Hofstetter W, Felix R, Fleisch HA, et al. c-Fos: a key regulator of osteoclast-macrophage lineage determination and bone remodeling. Science 1994; 266:443-8.
33. Li X, Udagawa N, Itoh K, Suda K, Murase Y, Nishihara T, et al. p38 MAPK-mediated signals are required for inducing osteoclast differentiation but not for osteoclast function. Endocrinology 2002;143:3105-13.
34. Shiotani A, Takami M, Itoh K, Shibasaki Y, Sasaki T. Regulation of osteoclast differentiation and function by receptor activator of NFkB ligand and osteoprotegerin. Anat Rec 2002;268:137-46.
35. Takayanagi H, Kim S, Koga T, Nishina H, Isshiki M, Yoshida H, et al. Induction and activation of the transcription factor NFATc1 (NFAT2) integrate RANKL signaling in terminal differentiation of osteoclasts. Dev Cell 2002;3:889-901.
36. Yamashita T, Yao Z, Li F, Zhang Q, Badell IR, Schwarz EM, et al. NF-kappaB p50 and p52 regulate receptor activator of NF-kappaB ligand (RANKL) and tumor necrosis factor-induced osteoclast precursor differentiation by activating c-Fos and NFATc1. J Biol Chem 2007;282:18245-53.
37. Ishida N, Hayashi K, Hoshijima M, Ogawa T, Koga S, Miyatake Y, et al. Large scale gene expression analysis of osteoclastogenesis in vitro and elucidation of NFAT2 as a key regulator. J Biol Chem 2002;277:41147-56.
38. van den Berg WB, van Lent PL, Joosten LA, Abdollahi-Roodsaz S, Koenders MI. Amplifying elements of arthritis and joint destruction. Ann Rheum Dis 2007;66 Suppl 3:iii45-8.
39. Scrivo R, Di Franco M, Spadaro A, Valesini G. The immunology of rheumatoid arthritis. Ann NY Acad Sci 2007;1108:312-22.
40. Lloyd M. Treatment of postmenopausal osteoporosis. N Engl J Med 1998;339:202; author reply 3.
41. Rodan GA, Martin TJ. Therapeutic approaches to bone diseases. Science 2000;289:1508-14.
42. O'Regan RM, Gradishar WJ. Selective estrogen-receptor modulators in 2001. Oncology (Williston Park) 2001;15:1177-85, 89-90; discussion 90-4.
43. Body JJ. Calcitonin for the long-term prevention and treatment of postmenopausal osteoporosis. Bone 2002;30:75S-9S.
44. Tremollieres F, Lopes P. [Specific estrogen receptor modulators (SERMs)]. Presse Med 2002;31:1323-8.
45. Watts NB. Bisphosphonate treatment of osteoporosis. Clin Geriatr Med 2003;19:395-414.
46. Lukhoba CW, Simmonds MS, Paton AJ. Plectranthus: a review of ethnobotanical uses. J Ethnopharmacol 2006;103:1-24.
47. Peake PW, Pussell BA, Martyn P, Timmermans V, Charlesworth JA. The inhibitory effect of rosmarinic acid on complement involves the C5 convertase. Int J Immunopharmacol 1991;13:853-7.
48. Osakabe N, Takano H, Sanbongi C, Yasuda A, Yanagisawa R, Inoue K, et al. Anti-inflammatory and anti-allergic effect of rosmarinic acid (RA); inhibition of seasonal allergic rhinoconjunctivitis (SAR) and its mechanism. Biofactors 2004;21:127-31.
49. Youn J, Lee KH, Won J, Huh SJ, Yun HS, Cho WG, et al. Beneficial effects of rosmarinic acid on suppression of collagen induced arthritis. J Rheumatol 2003;30:1203-7.
50. Schett G, Stolina M, Bolon B, Middleton S, Adlam M, Brown H, et al. Analysis of the kinetics of osteoclastogenesis in arthritic rats. Arthritis Rheum 2005;52:3192-201.
51. Dougall WC, Glaccum M, Charrier K, Rohrbach K, Brasel K, De Smedt T, et al. RANK is essential for osteoclast and lymph node development. Genes Dev 1999;13:2412-24.
52. Kong YY, Yoshida H, Sarosi I, Tan HL, Timms E, Capparelli C, et al. OPGL is a key regulator of osteoclastogenesis, lymphocyte development and lymph-node organogenesis. Nature 1999; 397:315-23.
53. Luo JL, Kamata H, Karin M. IKK/NF-kappa B signaling: balancing life and death — a new approach to cancer therapy. J Clin Invest 2005;115:2625-32.
54. Crotti TN, Flannery M, Walsh NC, Fleming JD, Goldring SR, McHugh KP. NFATc1 regulation of the human beta3 integrin promoter in osteoclast differentiation. Gene 2006;372:92-102.
55. Matsumoto M, Kogawa M, Wada S, Takayanagi H, Tsujimoto M, Katayama S, et al. Essential role of p38 mitogen-activated protein kinase in cathepsin K gene expression during osteoclastogenesis through association of NFATc1 and PU.1. J Biol Chem 2004;279:45969-79.
56. Feldmann M, Brennan FM, Maini RN. Role of cytokines in rheumatoid arthritis. Annu Rev Immunol 1996;14:397-440.
57. Andreakos ET, Foxwell BM, Brennan FM, Maini RN, Feldmann M. Cytokines and anti-cytokine biologicals in autoimmunity: present and future. Cytokine Growth Factor Rev 2002;13:299-313.